

Search for pentaquark states in Z decays

S. Schael, R. Barate, R. Bruneliere, I. de Bonis, D. Decamp, C. Goy, S. Jezequel, J P. Lees, F. Martin, E. Merle, et al.

► **To cite this version:**

S. Schael, R. Barate, R. Bruneliere, I. de Bonis, D. Decamp, et al.. Search for pentaquark states in Z decays. Physics Letters B, Elsevier, 2004, 599, pp.1-16. 10.1016/j.physletb.2004.08.021 . in2p3-00021800

HAL Id: in2p3-00021800

<http://hal.in2p3.fr/in2p3-00021800>

Submitted on 10 Sep 2004

HAL is a multi-disciplinary open access archive for the deposit and dissemination of scientific research documents, whether they are published or not. The documents may come from teaching and research institutions in France or abroad, or from public or private research centers.

L'archive ouverte pluridisciplinaire **HAL**, est destinée au dépôt et à la diffusion de documents scientifiques de niveau recherche, publiés ou non, émanant des établissements d'enseignement et de recherche français ou étrangers, des laboratoires publics ou privés.

Search for pentaquark states in Z decays

The ALEPH Collaboration¹

Abstract

Exotic hadrons made of five quarks (pentaquarks) are searched for in hadronic Z decays collected by the ALEPH detector at LEP. No significant signal is observed. At 95% C.L., upper limits are set on the production rates N of such particles and their charge-conjugate state per Z decay:

$$\begin{aligned}
N_{\Theta(1535)^+} \cdot \text{BR}(\Theta(1535)^+ \rightarrow \text{pK}_S^0) &< 6.2 \times 10^{-4}, \\
N_{\Xi(1862)^{--}} \cdot \text{BR}(\Xi(1862)^{--} \rightarrow \Xi^- \pi^-) &< 4.5 \times 10^{-4}, \\
N_{\Xi(1862)^0} \cdot \text{BR}(\Xi(1862)^0 \rightarrow \Xi^- \pi^+) &< 8.9 \times 10^{-4}, \\
N_{\Theta_c(3100)^0} \cdot \text{BR}(\Theta_c(3100)^0 \rightarrow \text{D}^{*-} \text{p}) &< 6.3 \times 10^{-4}, \\
N_{\Theta_c(3100)^0} \cdot \text{BR}(\Theta_c(3100)^0 \rightarrow \text{D}^- \text{p}) &< 31 \times 10^{-4}.
\end{aligned}$$

Submitted to *Physics Letters B*

¹See next pages for the list of authors.

The ALEPH Collaboration

S. Schael

Physikalisches Institut der RWTH-Aachen, D-52056 Aachen, Germany

R. Barate, R. Brunelière, I. De Bonis, D. Decamp, C. Goy, S. Jézéquel, J.-P. Lees, F. Martin, E. Merle, M.-N. Minard, B. Pietrzyk, B. Trocmé

Laboratoire de Physique des Particules (LAPP), IN²P³-CNRS, F-74019 Annecy-le-Vieux Cedex, France

S. Bravo, M.P. Casado, M. Chmeissani, J.M. Crespo, E. Fernandez, M. Fernandez-Bosman, Ll. Garrido,¹⁵ M. Martinez, A. Pacheco, H. Ruiz

Institut de Física d'Altes Energies, Universitat Autònoma de Barcelona, E-08193 Bellaterra (Barcelona), Spain⁷

A. Colaleo, D. Creanza, N. De Filippis, M. de Palma, G. Iaselli, G. Maggi, M. Maggi, S. Nuzzo, A. Ranieri, G. Raso,²⁴ F. Ruggieri, G. Selvaggi, L. Silvestris, P. Tempesta, A. Tricomi,³ G. Zito

Dipartimento di Fisica, INFN Sezione di Bari, I-70126 Bari, Italy

X. Huang, J. Lin, Q. Ouyang, T. Wang, Y. Xie, R. Xu, S. Xue, J. Zhang, L. Zhang, W. Zhao

Institute of High Energy Physics, Academia Sinica, Beijing, The People's Republic of China⁸

D. Abbaneo, T. Barklow,²⁶ O. Buchmüller,²⁶ M. Cattaneo, B. Clerbaux,²³ H. Drevermann, R.W. Forty, M. Frank, F. Gianotti, J.B. Hansen, J. Harvey, D.E. Hutchcroft,³⁰ P. Janot, B. Jost, M. Kado,² P. Mato, A. Moutoussi, F. Ranjard, L. Rolandi, D. Schlatter, G. Sguazzoni, F. Teubert, A. Valassi, I. Videau

European Laboratory for Particle Physics (CERN), CH-1211 Geneva 23, Switzerland

F. Badaud, S. Dessagne, A. Falvard,²⁰ D. Fayolle, P. Gay, J. Jousset, B. Michel, S. Monteil, D. Pallin, J.M. Pascolo, P. Perret

Laboratoire de Physique Corpusculaire, Université Blaise Pascal, IN²P³-CNRS, Clermont-Ferrand, F-63177 Aubière, France

J.D. Hansen, J.R. Hansen, P.H. Hansen, A.C. Kraan, B.S. Nilsson

Niels Bohr Institute, 2100 Copenhagen, DK-Denmark⁹

A. Kyriakis, C. Markou, E. Simopoulou, A. Vayaki, K. Zachariadou

Nuclear Research Center Demokritos (NRCD), GR-15310 Attiki, Greece

A. Blondel,¹² J.-C. Brient, F. Machefert, A. Rougé, H. Videau

Laboratoire Leprince-Ringuet, Ecole Polytechnique, IN²P³-CNRS, F-91128 Palaiseau Cedex, France

V. Ciulli, E. Focardi, G. Parrini

Dipartimento di Fisica, Università di Firenze, INFN Sezione di Firenze, I-50125 Firenze, Italy

A. Antonelli, M. Antonelli, G. Bencivenni, F. Bossi, G. Capon, F. Cerutti, V. Chiarella, P. Laurelli, G. Mannocchi,⁵ G.P. Murtas, L. Passalacqua

Laboratori Nazionali dell'INFN (LNF-INFN), I-00044 Frascati, Italy

J. Kennedy, J.G. Lynch, P. Negus, V. O'Shea, A.S. Thompson

Department of Physics and Astronomy, University of Glasgow, Glasgow G12 8QQ, United Kingdom¹⁰

S. Wasserbaech

Utah Valley State College, Orem, UT 84058, U.S.A.

R. Cavanaugh,⁴ S. Dhamotharan,²¹ C. Geweniger, P. Hanke, V. Hepp, E.E. Kluge, A. Putzer, H. Stenzel, K. Tittel, M. Wunsch¹⁹

Kirchhoff-Institut für Physik, Universität Heidelberg, D-69120 Heidelberg, Germany¹⁶

R. Beuselinck, W. Cameron, G. Davies, P.J. Dornan, M. Girone,¹ N. Marinelli, J. Nowell, S.A. Rutherford, J.K. Sedgbeer, J.C. Thompson,¹⁴ R. White

Department of Physics, Imperial College, London SW7 2BZ, United Kingdom¹⁰

V.M. Ghete, P. Girtler, E. Kneringer, D. Kuhn, G. Rudolph

Institut für Experimentalphysik, Universität Innsbruck, A-6020 Innsbruck, Austria¹⁸

E. Bouhova-Thacker, C.K. Bowdery, D.P. Clarke, G. Ellis, A.J. Finch, F. Foster, G. Hughes, R.W.L. Jones, M.R. Pearson, N.A. Robertson, M. Smizanska

Department of Physics, University of Lancaster, Lancaster LA1 4YB, United Kingdom¹⁰

O. van der Aa, C. Delaere,²⁸ G. Leibenguth,³¹ V. Lemaitre²⁹

Institut de Physique Nucléaire, Département de Physique, Université Catholique de Louvain, 1348 Louvain-la-Neuve, Belgium

U. Blumenschein, F. Hölldorfer, K. Jakobs, F. Kayser, K. Kleinknecht, A.-S. Müller, B. Renk, H.-G. Sander, S. Schmeling, H. Wachsmuth, C. Zeitnitz, T. Ziegler

Institut für Physik, Universität Mainz, D-55099 Mainz, Germany¹⁶

A. Bonissent, P. Coyle, C. Curtil, A. Ealet, D. Fouchez, P. Payre, A. Tilquin

Centre de Physique des Particules de Marseille, Univ Méditerranée, IN²P³-CNRS, F-13288 Marseille, France

F. Ragusa

Dipartimento di Fisica, Università di Milano e INFN Sezione di Milano, I-20133 Milano, Italy.

A. David, H. Dietl,³² G. Ganis,²⁷ K. Hüttmann, G. Lütjens, W. Männer³², H.-G. Moser, R. Settles, M. Villegas, G. Wolf

Max-Planck-Institut für Physik, Werner-Heisenberg-Institut, D-80805 München, Germany¹⁶

J. Boucrot, O. Callot, M. Davier, L. Duflot, J.-F. Grivaz, Ph. Heusse, A. Jacholkowska,⁶ L. Serin, J.-J. Veillet

Laboratoire de l'Accélérateur Linéaire, Université de Paris-Sud, IN²P³-CNRS, F-91898 Orsay Cedex, France

P. Azzurri, G. Bagliesi, T. Boccali, L. Foà, A. Giammanco, A. Giassi, F. Ligabue, A. Messineo, F. Palla, G. Sanguinetti, A. Sciabà, P. Spagnolo, R. Tenchini, A. Venturi, P.G. Verdini

Dipartimento di Fisica dell'Università, INFN Sezione di Pisa, e Scuola Normale Superiore, I-56010 Pisa, Italy

O. Awunor, G.A. Blair, G. Cowan, A. Garcia-Bellido, M.G. Green, T. Medcalf, A. Misiejuk, J.A. Strong, P. Teixeira-Dias

Department of Physics, Royal Holloway & Bedford New College, University of London, Egham, Surrey TW20 OEX, United Kingdom¹⁰

R.W. Clift, T.R. Edgecock, P.R. Norton, I.R. Tomalin, J.J. Ward

Particle Physics Dept., Rutherford Appleton Laboratory, Chilton, Didcot, Oxon OX11 0QX, United Kingdom¹⁰

B. Bloch-Devauux, D. Boumediene, P. Colas, B. Fabbro, E. Lançon, M.-C. Lemaire, E. Locci, P. Perez, J. Rander, B. Tuchming, B. Vallage

CEA, DAPNIA/Service de Physique des Particules, CE-Saclay, F-91191 Gif-sur-Yvette Cedex, France¹⁷

A.M. Litke, G. Taylor

Institute for Particle Physics, University of California at Santa Cruz, Santa Cruz, CA 95064, USA²²

C.N. Booth, S. Cartwright, F. Combley,²⁵ P.N. Hodgson, M. Lehto, L.F. Thompson

Department of Physics, University of Sheffield, Sheffield S3 7RH, United Kingdom¹⁰

A. Böhrer, S. Brandt, C. Grupen, J. Hess, A. Ngac, G. Prange

Fachbereich Physik, Universität Siegen, D-57068 Siegen, Germany¹⁶

C. Borean, G. Giannini

Dipartimento di Fisica, Università di Trieste e INFN Sezione di Trieste, I-34127 Trieste, Italy

H. He, J. Putz, J. Rothberg

Experimental Elementary Particle Physics, University of Washington, Seattle, WA 98195 U.S.A.

S.R. Armstrong, K. Berkelman, K. Cranmer, D.P.S. Ferguson, Y. Gao,¹³ S. González, O.J. Hayes, H. Hu, S. Jin, J. Kile, P.A. McNamara III, J. Nielsen, Y.B. Pan, J.H. von Wimmersperg-Toeller, W. Wiedenmann, J. Wu, Sau Lan Wu, X. Wu, G. Zobernig

Department of Physics, University of Wisconsin, Madison, WI 53706, USA¹¹

G. Dissertori

Institute for Particle Physics, ETH Höggerberg, 8093 Zürich, Switzerland.

¹Also at CERN, 1211 Geneva 23, Switzerland.

²Now at Fermilab, PO Box 500, MS 352, Batavia, IL 60510, USA

³Also at Dipartimento di Fisica di Catania and INFN Sezione di Catania, 95129 Catania, Italy.

⁴Now at University of Florida, Department of Physics, Gainesville, Florida 32611-8440, USA

⁵Also IFSI sezione di Torino, CNR, Italy.

⁶Also at Groupe d'Astroparticules de Montpellier, Université de Montpellier II, 34095, Montpellier, France.

⁷Supported by CICYT, Spain.

⁸Supported by the National Science Foundation of China.

⁹Supported by the Danish Natural Science Research Council.

¹⁰Supported by the UK Particle Physics and Astronomy Research Council.

¹¹Supported by the US Department of Energy, grant DE-FG0295-ER40896.

¹²Now at Département de Physique Corpusculaire, Université de Genève, 1211 Genève 4, Switzerland.

¹³Also at Department of Physics, Tsinghua University, Beijing, The People's Republic of China.

¹⁴Supported by the Leverhulme Trust.

¹⁵Permanent address: Universitat de Barcelona, 08208 Barcelona, Spain.

¹⁶Supported by Bundesministerium für Bildung und Forschung, Germany.

¹⁷Supported by the Direction des Sciences de la Matière, C.E.A.

¹⁸Supported by the Austrian Ministry for Science and Transport.

¹⁹Now at SAP AG, 69185 Walldorf, Germany

²⁰Now at Groupe d'Astroparticules de Montpellier, Université de Montpellier II, 34095 Montpellier, France.

²¹Now at BNP Paribas, 60325 Frankfurt am Mainz, Germany

²²Supported by the US Department of Energy, grant DE-FG03-92ER40689.

²³Now at Institut Inter-universitaire des hautes Energies (IHE), CP 230, Université Libre de Bruxelles, 1050 Bruxelles, Belgique

²⁴Now at Dipartimento di Fisica e Tecnologia Relative, Università di Palermo, Palermo, Italy.

²⁵Deceased.

²⁶Now at SLAC, Stanford, CA 94309, U.S.A

²⁷Now at CERN, 1211 Geneva 23, Switzerland

²⁸Research Fellow of the Belgium FNRS

²⁹Research Associate of the Belgium FNRS

³⁰Now at Liverpool University, Liverpool L69 7ZE, United Kingdom

³¹Supported by the Federal Office for Scientific, Technical and Cultural Affairs through the Interuniversity Attraction Pole P5/27

³²Now at Henryk Niewodniczski Institute of Nuclear Physics, Polish Academy of Sciences, Cracow, Poland

1 Introduction

Although Quantum Chromodynamics (QCD) does not a priori exclude other stable configurations of quarks and gluons, observations had until recently revealed only very few hadronic states with quantum numbers that could not be explained as bound states of two or three (anti-)quarks. During 2003, however, a large body of experimental evidence was presented for the existence of hadronic states that cannot be explained in this picture.

The first observation was that of a narrow resonance at $1540 \pm 10 \text{ MeV}/c^2$, named Θ^+ , produced in the reaction $\gamma n \rightarrow K^- \Theta^+$ followed by $\Theta^+ \rightarrow K^+ n$ [1]. This observation was confirmed by many experiments at different laboratories [2-9]. The observed masses range from 1521 to 1555 MeV/c^2 with an average of about 1535 MeV/c^2 . Furthermore, all experiments find a resonance width consistent with the experimental mass resolution. From $K^+ n$ scattering data, an upper limit of about 2 MeV has been set on the Θ^+ natural width [10]. The resonance is a baryon with positive strangeness, which is inexplicable in the three-quark model, but possible in a pentaquark interpretation (uudd \bar{s}).

Shortly after, another exotic baryon, doubly-charged and doubly-strange ($\Xi(1862)^{--}$), was reported by the CERN experiment NA49 [11]. Recently, the DESY experiment H1 has reported a signal for a charmed exotic baryon, $\Theta_c(3100)$, in the pD^{*-} channel [12]. These two observations have, however, not been confirmed by other experiments.

The observed states agree with a prediction from the chiral soliton model [13]. Alternative explanations have also been proposed, invoking “molecules” of various tightly-coupled quark configurations [14-16]. The production mechanism could be quite unusual. For example, in the CLAS experiment, a strong contribution seems to come from the decay of a heavy excited neutron state with a mass around 2400 MeV/c^2 [5]. In order to shed more light on these possibilities, it is of interest to search for pentaquark states in e^+e^- reactions.

In this letter, exotic baryons are searched for in the fragmentation of quarks from four million hadronic Z decays recorded by the ALEPH experiment during the LEP 1 operation in the years 1991 to 1995. After a short description of the ALEPH detector in Section 2 and of the overall event selection in Section 3, the results of searches for narrow resonance decays in the pK , $\Xi\pi$ and pD final states are given in Sections 4, 5 and 6. The negative results from these searches are compared with positive signals for non-exotic states, such as the $\Lambda(1520)$, the $\Xi(1530)^0$ and the $D^*(2010)$. Throughout this letter, any reference to a hadronic system, such as pK^+ , implicitly includes its charge-conjugate state, $\bar{p}K^-$ in this case.

2 The ALEPH detector

The ALEPH detector is described in detail in Ref. [17] and its performance in Ref. [18]. Here, the performance of the tracking detector is of interest.

The tracking system consists of two layers of double-sided silicon vertex detector (VDET), an inner tracking chamber (ITC) and a time projection chamber (TPC), immersed in an axial magnetic field of 1.5 T provided by a superconducting solenoidal coil. The VDET single hit resolution is $12 \mu\text{m}$ at normal incidence for both the $r\phi$ and rz projections (r , ϕ and z are the cylindrical coordinates around the symmetry axis directed along the e^- beam). The polar angle coverage of the inner and outer layers is $|\cos\theta| < 0.84$ and $|\cos\theta| < 0.69$, respectively. The ITC provides up to eight $r\phi$ hits at radii between 16 and 26 cm with an average resolution of $150 \mu\text{m}$ and has an angular coverage down to $|\cos\theta| < 0.97$. The TPC measures up to 21 three-dimensional points per charged particle at radii between 40 and 171 cm, with an $r\phi$ resolution of $170 \mu\text{m}$, an rz resolution of $740 \mu\text{m}$ and with an angular coverage down to $|\cos\theta| < 0.97$.

Tracks are reconstructed using the TPC, ITC and VDET, with a transverse momentum resolution of $\sigma(1/p_T) = 6 \times 10^{-4} \oplus 5 \times 10^{-3}/p_T$ (GeV/c) $^{-1}$. In the following, good tracks are defined as charged-particle tracks reconstructed with at least four hits in the TPC, originating from within a cylinder of length 20 cm and radius 2 cm coaxial with the beam and centred at the nominal interaction point, and with a polar angle with respect to the beam such that $|\cos \theta| < 0.95$.

Good tracks are identified as electrons, pions, protons or kaons by the ionization energy loss, dE/dx , estimated using pulse height information from both the anode wires and the cathode pads at the TPC end-walls [19]. For the momenta of interest in this study, this estimator yields, above 2 GeV/c, a 2σ separation between pions and kaons and a 3σ separation between pions and protons. For momenta below 1 GeV/c, most particles can be unambiguously identified.

3 Event selection and particle identification

A pure sample of hadronic Z decays is obtained by selecting events with at least six good tracks, carrying at least 10% of the centre-of-mass energy. The thrust axis is required to have an angle to the beam axis exceeding 25° . A total of 3.5 million hadronic Z decays are retained, corresponding to 87% of the total hadronic cross section.

A particle of type i ($i = \pi, K, p$ or e) can be identified by the pull R_i defined by

$$R_i = \frac{dE/dx(\text{measured}) - dE/dx(\text{expected for hypothesis } i)}{\sigma(\text{expected for hypothesis } i)}.$$

To be selected as pions, kaons or protons, the particles must fulfil the momentum-dependent criteria displayed in Table 1. Among particles that originate within 2 mm of the reconstructed primary vertex, these criteria select, for example, 1.3 million proton candidates (5.4 million kaon candidates) with a purity of 52% (58%) in the high momentum range and 96% (83%) in the low momentum range.

Table 1: Selection criteria for charged pion, kaon and proton identification

Particle	Momentum (GeV/c)	R_π	$ R_K $	$ R_p $	$ R_e $
π	no cut	< 2.5	no cut	no cut	no cut
K	< 0.8	> 2.0	< 2.0	no cut	> 2.0
	> 1.5	< -1.5	< 2.0	no cut	no cut
p	< 1.2	> 2.5	no cut	< 2.0	> 2.0
	> 2.0	< -3.0	no cut	< 2.0	no cut

Pairs of oppositely-charged pion tracks are tested for the hypothesis that they are decay products of a K_S^0 created at the primary vertex [20]. The reconstructed proper decay time is required to exceed 10% of the K_S^0 lifetime. If the χ^2 of a mass-constrained fit is less than 20, the pair is selected. These criteria select 1.24 million K_S^0 candidates with a purity of 93%.

Candidates for $\Lambda \rightarrow p\pi^-$ decays are found by associating oppositely-charged pion and proton tracks. Each Λ is paired with a pion track that misses the beam axis by at least 2 mm. These pairs are tested for the hypothesis that they arise from the decay of a particle created at the primary vertex. The secondary vertex fit is required to yield a χ^2 smaller than 40. If this particle carries more than 2% of the beam momentum and has a reconstructed proper decay time in excess of 1% of the Ξ^- lifetime, it is retained as a Ξ candidate.

Finally, combinations of a kaon candidate with momentum exceeding 2.5 GeV/c together with one (or two) pions are tested for a common vertex. If such a vertex is found with a χ^2 less than 3

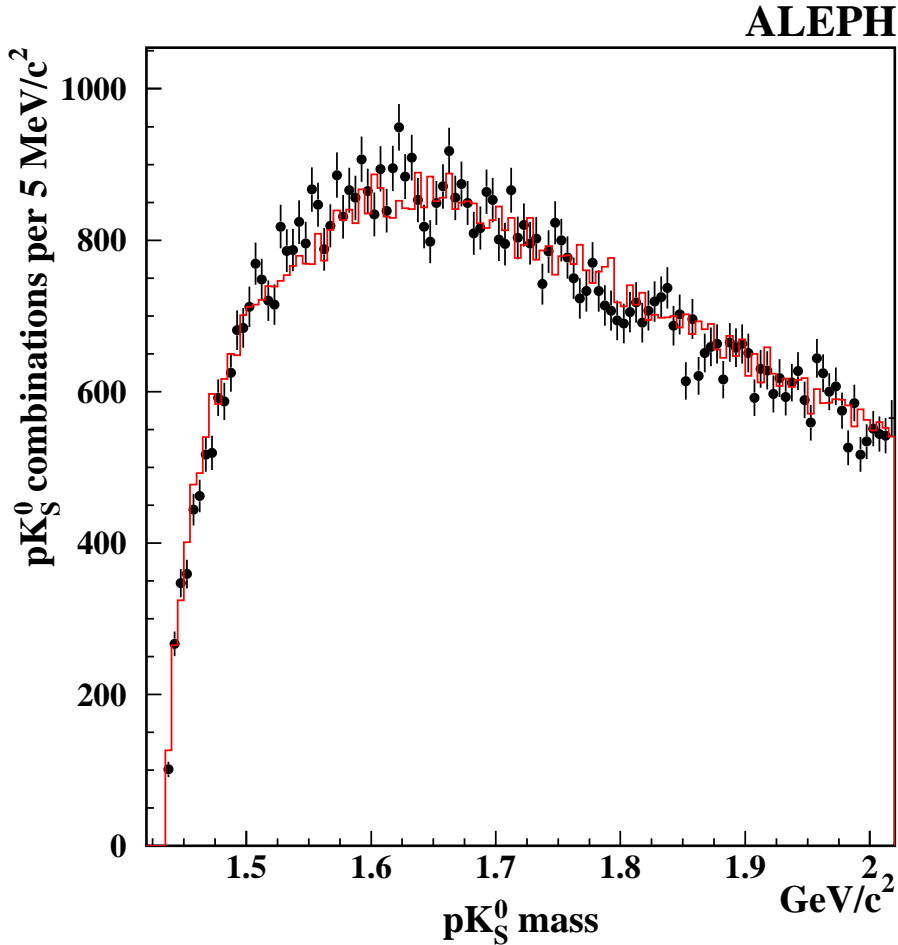


Figure 1: Mass distribution of pK_S^0 combinations, for the data (dots with error bars) and the simulation (histogram). The simulated distribution is normalized to the total number of combinations in the data.

(or 10) and is separated by more than 2σ from the primary vertex, the combination is tagged as a D meson candidate [21].

4 Search for narrow resonances in the pK system

The $\Theta(1535)^+$ was searched for as a narrow peak in the invariant mass of combinations of a reconstructed K_S^0 and a proton track, selected as described in Section 3. The selection retains 480 000 combinations (0.14 per Z decay) with a pK_S^0 purity of 50%. The mass distribution of the pK_S^0 combinations is displayed in Fig. 1 and is compared with the simulation from JETSET [22], with parameters hereof as determined in Ref. [23]. The simulation includes all octet and decuplet baryon ground states, but no other baryon resonances.

In the absence of a simulation of the $\Theta(1535)^+$ in Z decay, the mass resolution was deduced from width measurements of various known resonances with total kinetic energies of the decay products in the resonance rest frame (Q values) ranging from 30 to 300 MeV. For example, from the fitted Breit-Wigner width of 50.9 ± 0.7 MeV for the decay $K^*(892) \rightarrow \pi K_S^0$ ($Q = 255$ MeV), the mass resolution was deduced to be less than 5 MeV/ c^2 (Fig. 2a). Similarly, the resolution for $\Xi^- \rightarrow \Lambda \pi^-$ ($Q = 66$ MeV) was found to be 2.8 MeV/ c^2 and the resolution for $\phi \rightarrow K^+ K^-$ ($Q = 32$

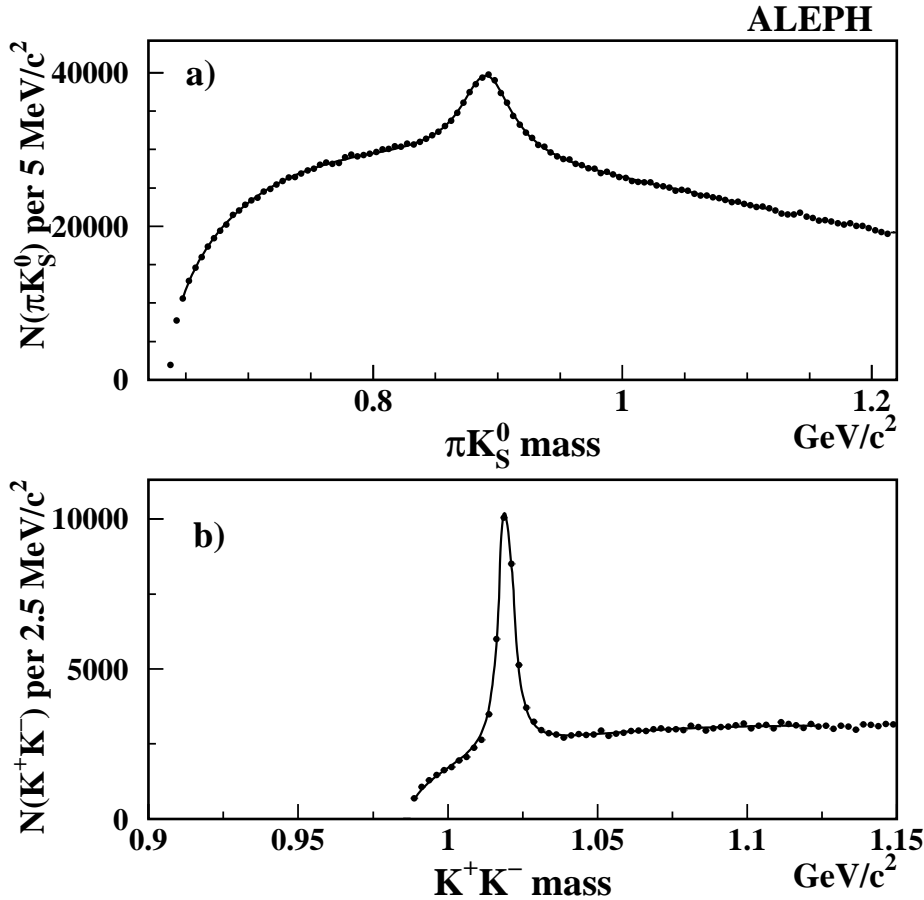


Figure 2: Mass distributions of (a) πK_S^0 and (b) K^+K^- combinations. The curve is a fit to the background parametrization of Eq. 1 with a Breit-Wigner function superimposed. These measurements were used to estimate the mass resolution for the $\Theta(1535)^+$.

MeV) was found to average $1.6 \text{ MeV}/c^2$ (Fig. 2b). Since the mass resolution is a rising function of the Q value, the average resolution for $\Theta^+ \rightarrow p K_S^0$ ($Q = 100 \text{ MeV}$) is expected to be $3\text{-}4 \text{ MeV}/c^2$ and is conservatively assumed to be smaller than $5 \text{ MeV}/c^2$ in the following.

The $\Theta(1535)^+$ resonance was searched for in the following way. First, the data in Fig. 1 were fitted by the function

$$f(M) = a_1(M - M_{\text{thr}})^{a_2} \exp(a_3 M), \quad (1)$$

where M_{thr} is the threshold mass (here, $M_{\text{thr}} = M_p + M_{K_S^0}$) and a_i are the fitted parameters. The signal was searched for as an excess with respect to the fit result, rather than to the simulation, because of the contribution from known but unsimulated Σ^* resonances in this mass range. An excess with respect to the fit was searched for in a $20\text{-MeV}/c^2$ -wide window sliding from 1500 to $1600 \text{ MeV}/c^2$. (This sliding window is excluded from the fit to the data.) The largest excess was found in the window between 1540 and $1560 \text{ MeV}/c^2$, and amounts to 49 above a fitted background of 3240 combinations.

To evaluate the upper limit on the production of $\Theta(1535)^+$ in hadronic Z decays, a large number of toy experiments were generated according to the fitted mass distribution. A resonance with

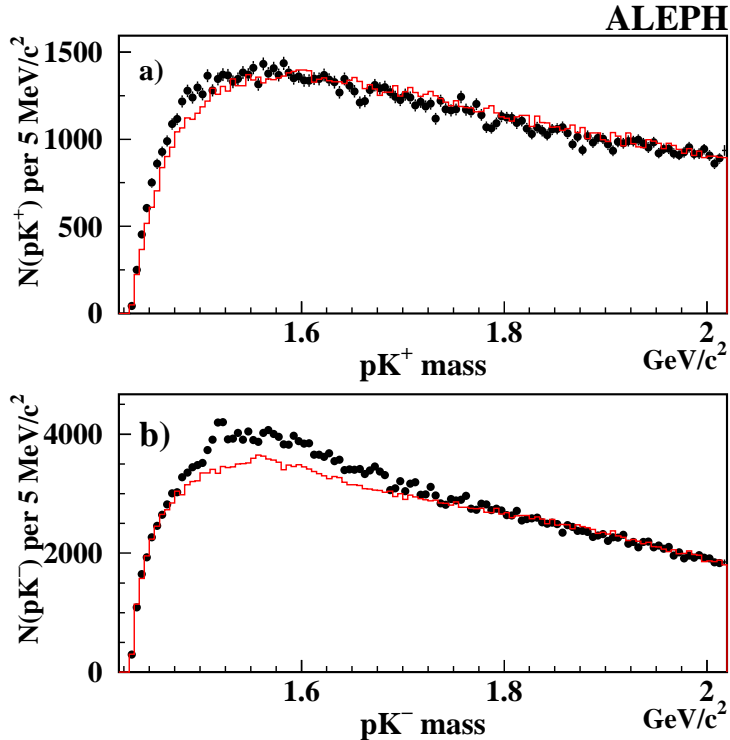


Figure 3: Mass distributions of (a) pK^+ and (b) pK^- combinations, for the data (dots with error bars) and the simulation (histogram). In (a) the simulation is normalized to the total number of combinations in the data. In (b) the simulation is corrected by the data-to-simulation ratio of (a) and normalized to the number of combinations in data with masses above $1.8 \text{ GeV}/c^2$.

mass resolution $5 \text{ MeV}/c^2$ and varying amplitude was thrown in, and the excess was determined as described above. The 95% C.L. upper limit on this amplitude is the value for which 5% of the toy experiments yield an excess smaller than 49, as observed in the data. This upper limit is found to be an average production of 151 combinations in the mass window.

In the mass range from 1500 to $1600 \text{ MeV}/c^2$, the efficiency to select pK_S^0 combinations was found to be $6.3 \pm 0.2\%$, the uncertainty being dominated by systematic uncertainties in the proton and K_S^0 selection. Once this efficiency is folded in, the 95% C.L. upper limit on the production rate times branching ratio of the $\Theta(1535)^+$ and its antiparticle per hadronic Z decay is found to be

$$N_{\Theta(1535)^+} \cdot \text{BR}(\Theta(1535)^+ \rightarrow pK_S^0) < 6.2 \times 10^{-4}.$$

The $\Theta^+ \rightarrow pK_S^0$ branching ratio is expected to be 25% from Ref. [7] and isospin arguments, which yields the upper limit on the production rate of

$$N_{\Theta(1535)^+} < 0.0025.$$

A cross check was performed with a search for doubly-charged (pK^+) and neutral (pK^-) combinations. No resonance structure is observed in the mass distribution of the doubly-charged pK combinations, shown in Fig. 3a. A smooth deviation of a few percent is seen with respect to the simulated spectrum. This deviation is a general feature of the simulation which is also present in combinations of oppositely-charged tracks. The observed data-to-simulation ratio in Fig. 3a was therefore used to correct the simulation of neutral pK combinations, as shown in Fig. 3b.

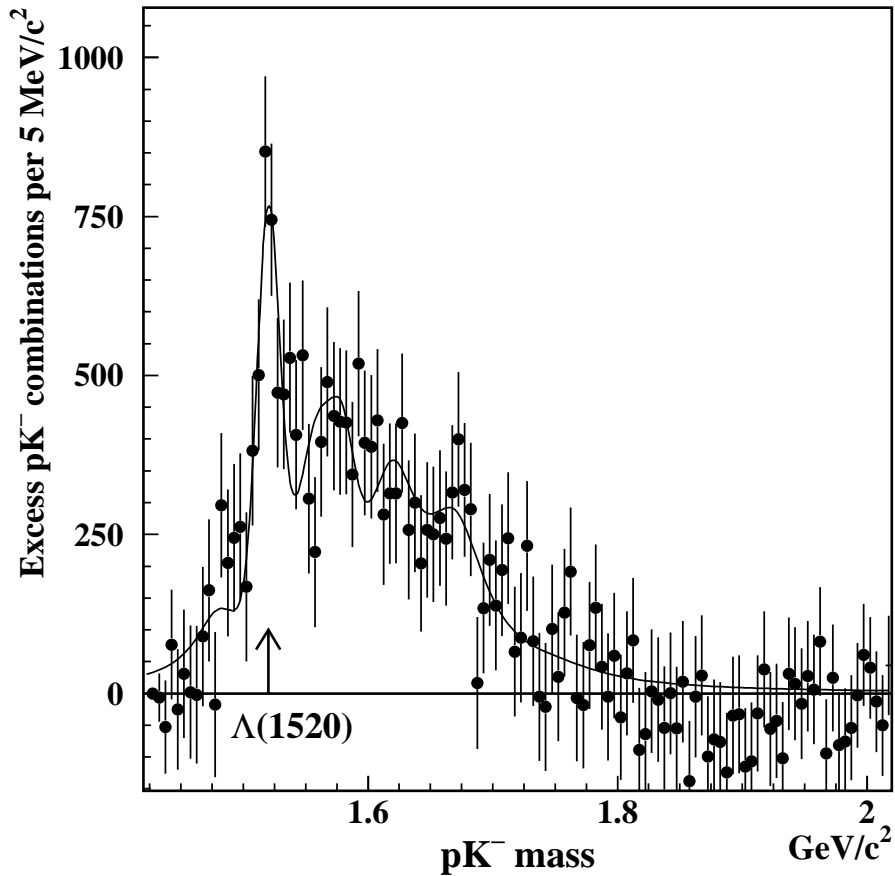


Figure 4: Mass distribution of pK^- combinations after subtraction of the simulated spectrum with a fit superimposed as explained in the text.

In the neutral pK combinations a clear resonance activity is visible in the mass range 1460 to 1800 MeV/c^2 , with a narrow peak due to the $\Lambda(1520)$ and a broad enhancement from many Σ^* resonances. A simultaneous fit to the amplitude of eight NK resonances ($\Lambda(1520)$, $\Sigma(1480)$, $\Sigma(1560)$, $\Sigma(1580)$, $\Sigma(1620)$, $\Sigma(1660)$, $\Sigma(1670)$ and $\Sigma(1750)$ [24]) over the corrected simulation is shown in Fig. 4. For the narrow states, $\Lambda(1520)$ and $\Sigma(1580)$, Gaussian contributions of 9 MeV/c^2 width are assumed. For the rest of the resonances, Breit-Wigner shaped contributions are assumed with widths of 45, 47, 50, 100, 60 and 90 MeV/c^2 , respectively.

The fit results in a $\Lambda(1520)$ contribution of 2874 ± 320 combinations. The systematic uncertainty on this result is estimated to be 270 combinations from varying the fit function and the normalization of the simulation.

With an average pK^- selection efficiency of $9.7 \pm 0.9\%$ (obtained from simulated kaons and protons in the mass range from 1500 to 1600 MeV/c^2) and a $\Lambda(1520) \rightarrow pK^-$ branching fraction of 22.5% [24], the production rate per hadronic Z decay of $\Lambda(1520)$ is found to be

$$N_{\Lambda(1520)} = 0.033 \pm 0.004 \pm 0.003,$$

in agreement with earlier measurements from OPAL [25] and DELPHI [26]. The resulting 95% C.L.

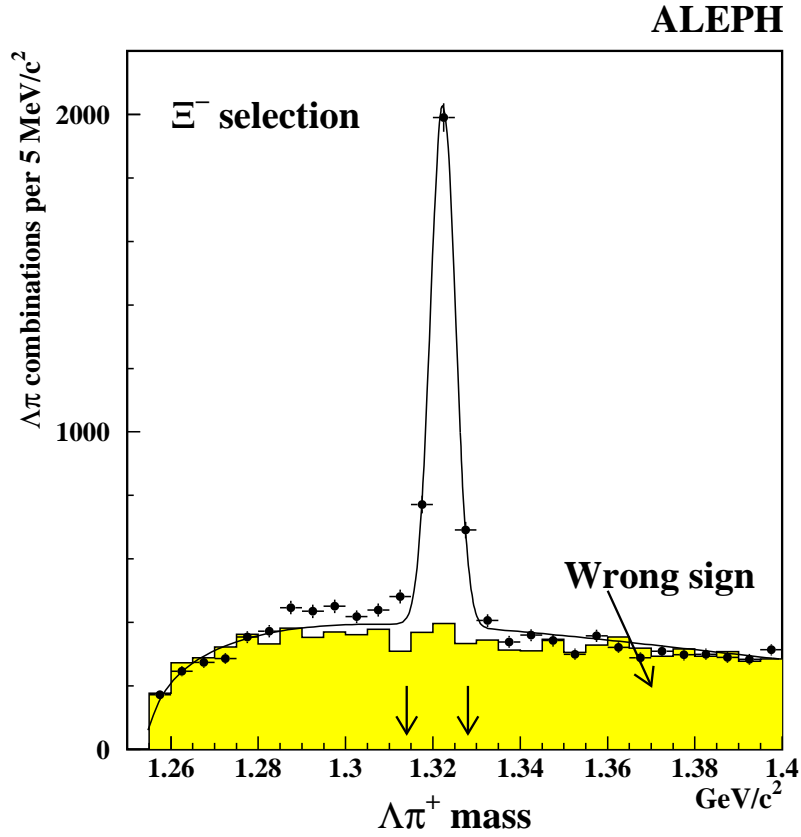


Figure 5: Mass distribution of $\Lambda\pi^-$ (dots) and $\Lambda\pi^+$ (shaded histogram) combinations in the data. The curve is a fit of the $\Lambda\pi^-$ mass distribution to Eq. 1 with a Gaussian function superimposed. The broad enhancement at low mass in the $\Lambda\pi^-$ channel is due to a non-Gaussian component in the mass resolution.

upper limit on the ratio of the Θ^+ to the $\Lambda(1520)$ production in Z decays is

$$\frac{N_{\Theta(1535)^+} \cdot \text{BR}(\Theta(1535)^+ \rightarrow pK_S^0)}{N_{\Lambda(1520)}} < 0.027,$$

if the $\Lambda(1520)$ production is fixed to the average value of the three measurements at LEP, i.e., 0.024 ± 0.002 per hadronic Z decay.

Subsets of the selected pK_S^0 sample were also considered. These subsets include combinations with high-purity proton candidates at momenta below $1 \text{ GeV}/c$, combinations with decay angles exceeding 37° with respect to the line of flight, combinations which, combined further with a K^- , could form an excited neutron state with a mass around $2400 \text{ MeV}/c^2$ and inclusive combinations in light quark decays of the Z. In none of these subsets was a significant $\Theta(1535)^+$ signal observed.

5 Search for narrow resonances in the $\Xi\pi$ system

A sample of Ξ^- candidates was reconstructed as explained in Section 3. A subsample of 3450 candidates was selected within $\pm 7 \text{ MeV}/c^2$ of the Ξ^- mass, as indicated by the vertical arrows in the $\Lambda\pi$ mass distribution shown in Fig. 5. This sample has a purity of 76%. Each Ξ candidate was combined with a charged pion to produce the mass spectra of the doubly-charged and neutral combinations of Fig. 6.

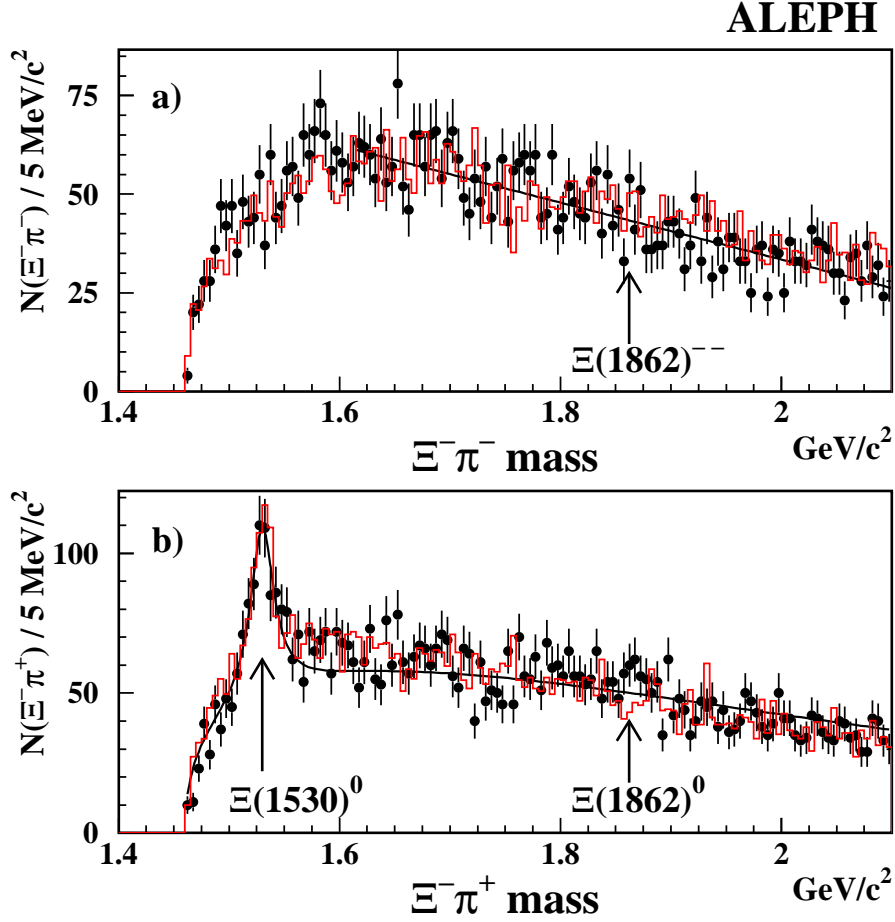


Figure 6: Mass distribution of (a) $\Xi^- \pi^-$ and (b) $\Xi^- \pi^+$ combinations, for the data (dots with error bars) and the simulation (histogram). The curves are fits to the data as explained in the text.

The mass spectrum of the doubly-charged combinations can be fitted to a function linearly decreasing with mass in the range from 1620 to 2100 MeV/c^2 . The mass resolution is estimated to be $6 \text{ MeV}/c^2$ from a simulation of the $\Xi(1530)^0$. The narrow resonance observed by NA49 [11] at 1862 MeV/c^2 is searched for in a 25- MeV/c^2 -wide mass window around this mass value as explained in Section 4. The number of $\Xi^- \pi^-$ combinations in this window amounts to 8 ± 15 in excess of the linear background fit. The 95% C.L. upper limit on a signal from a narrow resonance is evaluated to be 24 combinations in the window.

In the neutral channel ($\Xi^- \pi^+$), the data are described by Eq. 1 with a Breit-Wigner superimposed, centred at 1530 MeV/c^2 . An excess of 32 ± 16 is found in the same window, leading to an upper limit of 47 excess combinations. With a selection efficiency of $1.4 \pm 0.1\%$ ($1.5 \pm 0.1\%$) for $\Xi^- \pi^-$ ($\Xi^- \pi^+$) pairs simulated in the same mass range, 95% C.L. upper limits on the $\Xi(1862)$ production rate in hadronic Z decays can be set at

$$\begin{aligned} N_{\Xi(1862)^{--}} \cdot \text{BR}(\Xi(1862)^{--} \rightarrow \Xi^- \pi^-) &< 4.5 \times 10^{-4}, \\ N_{\Xi(1862)^0} \cdot \text{BR}(\Xi(1862)^0 \rightarrow \Xi^- \pi^+) &< 8.9 \times 10^{-4}. \end{aligned}$$

In Fig. 6b, a clear $\Xi(1530)^0$ peak is observed. A signal of 322 ± 33 combinations is counted in excess

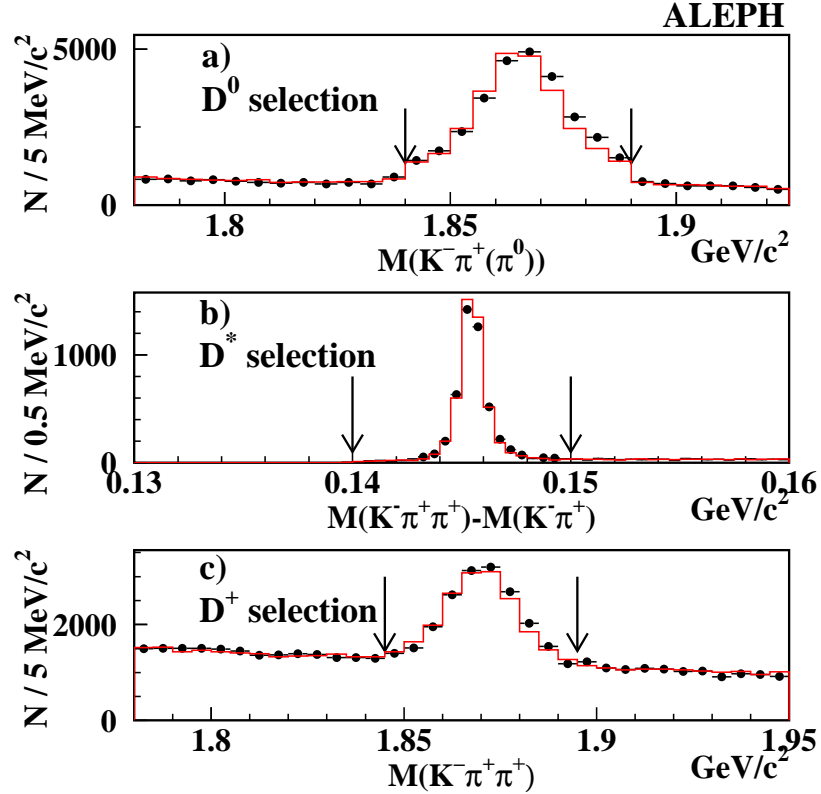


Figure 7: Selection of (a) D^0 , (b) D^* and (c) D^+ candidates. The dots are data and the histogram is simulation. The arrows indicate the selection cuts.

of the fitted background. With a selection efficiency of $1.56 \pm 0.14\%$ and an expected branching fraction into $\Xi^- \pi^+$ of 67%, the production rate per hadronic Z decay of $\Xi(1530)^0$ is found to be

$$N_{\Xi(1530)^0} = (77 \pm 8 \pm 6) \times 10^{-4},$$

in good agreement with published ALEPH [23] and OPAL results [25], whereas an earlier DELPHI measurement [27] finds a significantly lower production rate. The world average value of the $\Xi(1530)^0$ production rate, $(55 \pm 5) \times 10^{-4}$ allows 95% C.L. upper limits to be derived on the ratios:

$$\begin{aligned} N(\Xi(1862)^{--} \rightarrow \Xi^- \pi^-) / N(\Xi(1530)^0) &< 0.082, \\ N(\Xi(1862)^0 \rightarrow \Xi^- \pi^+) / N(\Xi(1530)^0) &< 0.16. \end{aligned}$$

6 Search for narrow resonances in the pD system

High-purity samples of D^0 and D^{*+} and a 50% pure sample of D^+ were selected as described in Section 3 and in greater detail in Ref. [21]. The corresponding mass distributions are shown in Fig. 7 with vertical arrows indicating the selected mass windows. On top of these selection criteria, D^0 and D^+ candidates were required to have momenta in excess of 7 and 14 GeV/c, respectively. Each $D^{(*)}$ candidate was paired in turn with each proton candidate in the event. The mass distributions of the pD * and pD combinations are shown in Fig. 8 and Fig. 9, respectively, in the mass range

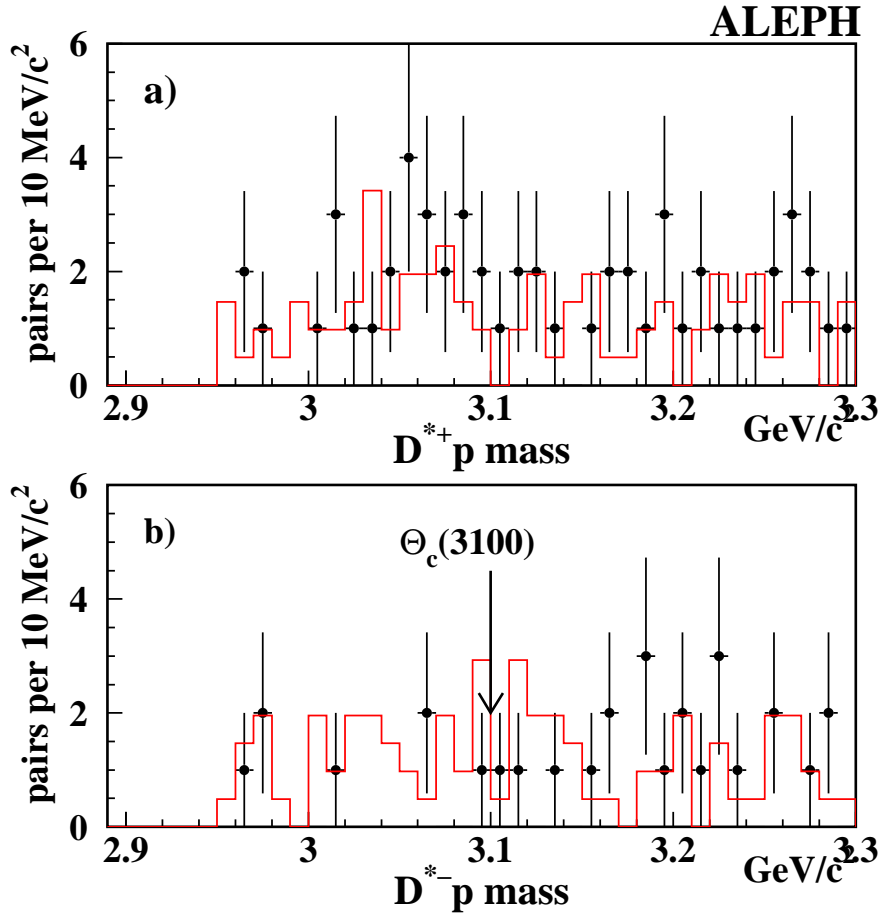


Figure 8: Invariant mass distribution of D^*p combinations, for the data (dots with error bars) and the simulation (histogram).

from 2.9 to 3.3 GeV/c^2 . As suggested in a previous ALEPH publication [28], the pD invariant mass was determined as

$$m_{pD} = m_{pD}^{\text{meas}} - m_D^{\text{meas}} + m_D^{\text{PDG}},$$

because the mass difference between the pD and the D systems is more accurately measured than the two individual masses. The resulting pD mass resolution was found to be about $3 \text{ MeV}/c^2$. The $\Theta_c(3100)^0$ signal observed by H1 [12] was located to within $\pm 3 \text{ MeV}/c^2$. Its Gaussian σ was determined to be $12 \pm 3 \text{ MeV}/c^2$ (consistent with the H1 mass resolution). A window of width $40 \text{ MeV}/c^2$ should therefore be adequate to cover any related enhancement.

The H1 experiment observed a signal in the pD^{*-} channel. In this channel, only three combinations are observed with an invariant mass between 3080 and 3120 MeV/c^2 , with 5.5 ± 0.5 combinations expected from a fit of Eq. 1 to the simulated background. In the pD^- channel, which was not covered by H1, the mass window is slid from threshold to 3120 MeV/c^2 . The most significant excess occurs in the mass window from 3080 to 3120 MeV/c^2 where 21 combinations are observed, with 17.5 ± 1.0 expected from the fit to the simulated background.

Channels with a charge different from that of the H1 signal are also shown. In Fig. 9c, an enhancement in the data is observed at 3140 MeV/c^2 in a 20- MeV/c^2 -wide mass interval. In

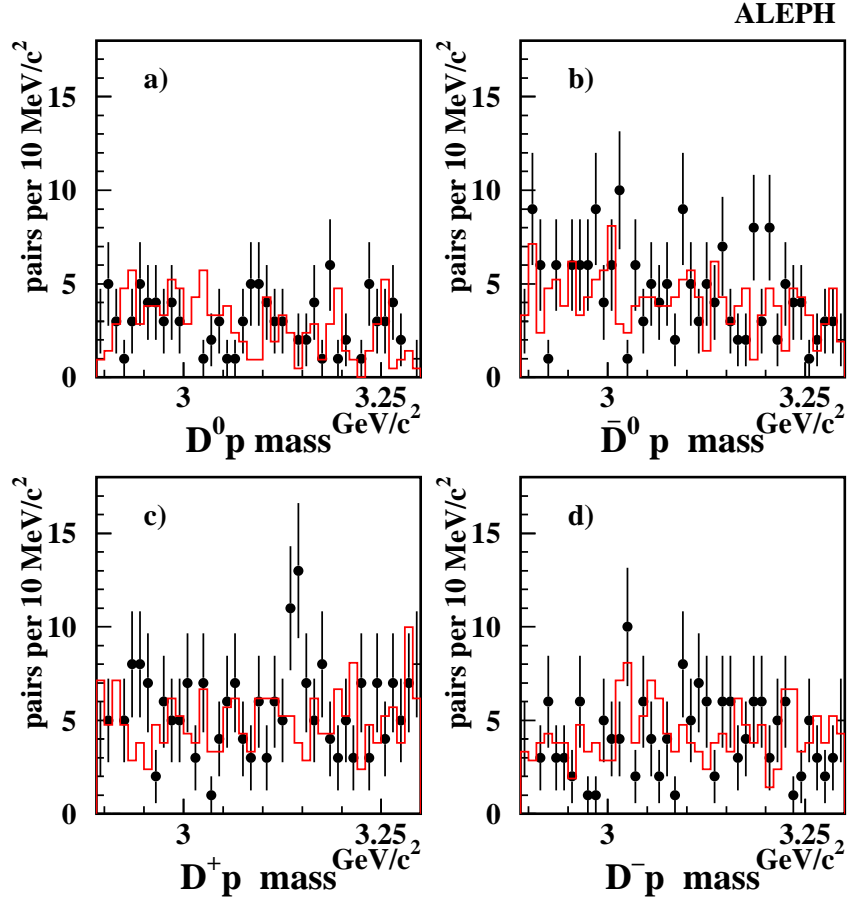


Figure 9: Invariant mass distributions of Dp combinations, for the data (dots with error bars) and the simulation (histogram).

this interval, 24 combinations are observed with 10.2 ± 0.5 expected from a fit of the simulated background. The probability for accidentally observing an enhancement of such significance in Fig. 9 is 5%.

The uncertainties in both the observed and expected number of combinations are dominated by limited statistics. The upper limit on the number of combinations coming from a new, narrow resonance in the mass window of interest is found by the methods described in Section 4.

With a reconstruction efficiency of 0.046 ± 0.004 (0.011 ± 0.001) and a visible branching ratio of 0.0259 ± 0.0006 (0.091 ± 0.006) for the pD^{*-} (pD^-) channel, upper limits on the $\Theta_c(3100)$ production rate are set at

$$\begin{aligned}
 N_{\Theta_c(3100)^0} \cdot \text{BR}(\Theta_c(3100)^0 \rightarrow D^{*-}p) &< 6.3 \times 10^{-4}, \\
 N_{\Theta_c(3100)^0} \cdot \text{BR}(\Theta_c(3100)^0 \rightarrow D^-p) &< 31 \times 10^{-4}.
 \end{aligned}$$

The 95% C.L. upper limit on the ratio of $\Theta_c(3100)^0$ to the D^* and D production in hadronic Z

decays is

$$\begin{aligned}\frac{N_{\Theta_c(3100)^0}}{N_{D^{*-}}} \cdot \text{BR}(\Theta_c(3100)^0 \rightarrow D^{*-}p) &< 0.0031, \\ \frac{N_{\Theta_c(3100)^0}}{N_{D^-}} \cdot \text{BR}(\Theta_c(3100)^0 \rightarrow D^-p) &< 0.018.\end{aligned}$$

if the D^* and D meson production is fixed to the world averages [24].

7 Conclusions

No evidence for exotic narrow baryon resonances has been found in the $e^+e^- \rightarrow Z \rightarrow q\bar{q}$ reactions collected by ALEPH during the LEP 1 running period. Upper limits at the 95% confidence level have been set on the production rates per hadronic Z decay of the resonances reported by other experiments:

$$\begin{aligned}N_{\Theta(1535)^+} \cdot \text{BR}(\Theta(1535)^+ \rightarrow pK_S^0) &< 6.2 \times 10^{-4}; \\ N_{\Xi(1862)^{--}} \cdot \text{BR}(\Xi_{1862}^{--} \rightarrow \Xi^- \pi^-) &< 4.5 \times 10^{-4}; \\ N_{\Xi(1862)^0} \cdot \text{BR}(\Xi_{1862}^0 \rightarrow \Xi^- \pi^+) &< 8.9 \times 10^{-4}; \\ N_{\Theta_c(3100)^0} \cdot \text{BR}(\Theta_c(3100)^0 \rightarrow D^{*-}p) &< 6.3 \times 10^{-4}; \\ N_{\Theta_c(3100)^0} \cdot \text{BR}(\Theta_c(3100)^0 \rightarrow D^-p) &< 31 \times 10^{-4}.\end{aligned}$$

The ratios to the production rates of the related non-exotic states are also bounded from above at the 95% confidence level by

$$\begin{aligned}\frac{N_{\Theta(1535)^+} \cdot \text{BR}(\Theta(1535)^+ \rightarrow pK_S^0)}{N_{\Lambda(1520)}} &< 0.027; \\ \frac{N_{\Xi(1862)^{--}}}{N_{\Xi(1530)^0}} \cdot \text{BR}(\Xi_{1862}^{--} \rightarrow \Xi^- \pi^-) &< 0.082; \\ \frac{N_{\Xi(1862)^0}}{N_{\Xi(1530)^0}} \cdot \text{BR}(\Xi_{1862}^0 \rightarrow \Xi^- \pi^+) &< 0.16; \\ \frac{N_{\Theta_c(3100)^0}}{N_{D^{*-}}} \cdot \text{BR}(\Theta_c(3100)^0 \rightarrow D^{*-}p) &< 0.0031; \\ \frac{N_{\Theta_c(3100)^0}}{N_{D^-}} \cdot \text{BR}(\Theta_c(3100)^0 \rightarrow D^-p) &< 0.018.\end{aligned}$$

The charge-conjugate states are included in these limits.

Acknowledgements

We wish to thank our colleagues from the CERN accelerator divisions for the successful operation of LEP. We are indebted to the engineers and technicians in all our institutions for their support in constructing and maintaining the ALEPH experiment. Those of us from non-member states thank CERN for its hospitality.

References

- [1] T.Nakano *et al.*, Phys. Rev. Lett. **91** (2003) 012002.
- [2] The DIANA Coll., *Observation of a baryon resonance with positive strangeness in K^+ collisions with Xe nuclei*, Phys. Atom. Nucl. **66**, (2003) 1715; Yad. Fiz. **66** (2003) 1763.
- [3] A. E. Asratyan, A. Dogolenko and M. A. Kubantsev, Phys. Atom. Nucl. **67** (2004) 682.
- [4] The CLAS Coll., *Observation of an exotic $S = +1$ baryon in exclusive photoproduction from the deuteron*, Phys. Rev. Lett. **91** (2003) 252001.
- [5] The CLAS Coll., *Observation of an exotic $S = +1$ baryon in exclusive photoproduction from the proton*, Phys. Rev. Lett. **92** (2004) 032001. Erratum-ibid 049902.
- [6] The SAPHIR Coll., *Evidence for the positive-strangeness pentaquark Θ^+ in photoproduction with the SAPHIR detector*, Phys. Lett. **B572** (2003) 127.
- [7] The HERMES Coll., *Evidence for a narrow $|S| = 1$ baryon state at a mass of 1528 MeV in quasireal photoproduction*, Phys. Lett. **B585** (2004) 213.
- [8] The SVD Coll., *Observation of a narrow baryon resonance decaying into pK_S^0 in pA interactions at 70 GeV/c with the SVD-2 setup*, hep-ex0401024, subm. to Yad. Fiz.
- [9] The ZEUS Coll., *Evidence for a narrow baryonic state decaying to $K_S^0 p$ and $K_S^0 \bar{p}$ in deep inelastic scattering at HERA*, Phys. Lett. **B591** (2004) 7.
- [10] R. Arndt, I. Strakovsky and R. Workman, Phys. Rev. **C68** (2003) 042201.
R. N. Cahn and G. H. Trilling, Phys. Rev. **D69** (2004) 011501.
- [11] The NA49 Coll., *Observation of an exotic $S = -2$, $Q = -2$ baryon resonance in proton-proton collisions at the CERN SPS*, Phys. Rev. Lett. **92** (2004) 042003.
- [12] The H1 Coll., *Evidence for a narrow anti-charmed baryon state*, Phys. Lett. **B588** (2004) 17.
- [13] D. Diakonov, V. Petrov and M. Polyakov, Z. Phys. **A359** (1997) 305.
- [14] S. Capstick *et al.*, Phys. Lett. **B570** (2003) 185.
- [15] M. Karliner and H. J. Lipkin, Phys. Lett. **B575** (2003) 249.
- [16] R. Jaffe and F. Wilczek, Phys. Rev. Lett **91** (2003) 232003.
- [17] The ALEPH Coll., *A Detector for Electron-Positron Annihilations at LEP*, Nucl. Instrum. and Methods **A294** (1990) 121.
- [18] The ALEPH Coll., *Performance of the ALEPH detector at LEP*, Nucl. Instrum. and Methods **A360** (1995) 481.
- [19] The ALEPH Coll., *Measurement of the anti- B^0 and B^- meson lifetimes*, Phys. Lett. **B492** (2000) 275.
- [20] The ALEPH Coll., *Production of K^0 and Λ in hadronic Z decays*, Z. Phys. **C64** (1994) 361.
- [21] The ALEPH Coll., *Study of charm production in Z decays*, Eur. Phys. J. **C16** (2000) 597.
- [22] T. Sjöstrand, Comp. Phys. Commun. **82** (1994) 74.

- [23] The ALEPH Coll., *Studies of Quantum Chromodynamics with the ALEPH detector*, Phys. Rep. **294** (1998) 1.
- [24] K. Hagiwara *et al.* (Particle Data Group), Phys. Rev. **D66** (2002) 010001.
- [25] The OPAL Coll., *Strange baryon production in hadronic Z decays*, Z. Phys. **C73** (1997) 569.
- [26] The DELPHI Coll., *Inclusive Σ^- and $\Lambda(1520)$ production in hadronic Z decays*, Phys. Lett. **B475** (2000) 429.
- [27] The DELPHI Coll., *Strange baryon production in hadronic Z decays*, Z. Phys. **C67** (1995) 543.
- [28] The ALEPH Coll., *Production of D_s^{**} in hadronic Z decays*, Phys. Lett. **B526** (2002) 34.